



Original Article

Phonon Characterization, Structural and Optical Properties of Type-II CdSe/CdTe core/shell and Type-II/type-I CdSe/CdTe/ZnS core/shell/shell Quantum Dots

Nguyen Xuan Ca*, Nguyen Thi Hien

Faculty of Physics, Thai Nguyen University of Sciences, Tan Thinh, Thai Nguyen, Viet Nam

Received 09 January 2020

Revised 17 February 2020; Accepted 05 April 2020

Abstract: The CdSe, type-II CdSe/CdTe core/shell and type-II/type-I CdSe/CdTe/ZnS core/shell/shell quantum dots (QDs) were successfully synthesized in a noncoordinating solvent. The phonon characterizations, optical properties and structures of the synthesized QDs were characterized by Raman scattering (RS) spectra, photoluminescence (PL) spectroscopy, PL-decay lifetime, absorption spectroscopy (Abs), and X-ray diffraction (XRD). The growth of QDs was monitored by using RS, which demonstrated the formation of correct of the core/shell and core/shell/shell structures. Observation results from XRD reveal that all QDs crystallize in the cubic phase with zinc-blende structure. The typical characteristics of spatially indirect recombination for type-II QDs were observed through Abs and PL spectroscopy. The ZnS shell significantly enhanced the PL quantum yield (QY), the optical durability, the chemical stability and separating CdSe/CdTe QDs from the surroundings. The effect of excitation power on the PL properties of the CdSe core, CdSe/CdTe and CdSe/CdTe/ZnS QDs has been investigated.

Keywords: Quantum dot, type-II/type-I, optical properties, photoluminescence.

1. Introduction

Colloidal semiconductors quantum dots (QDs) have been widely proposed to be used in applications such as light-emitting devices, lasers, photovoltaic and biomedical fluorescent labels because of the many desirable properties [1, 2]. They have many advantages compared to organic fluorescence such as tunable emission wavelength, multiplexing capabilities, high-photoluminescence

* Corresponding author.

Email address: canx@tnus.edu.vn

[https://doi.org/ 10.25073/2588-1124/vnumap.4452](https://doi.org/10.25073/2588-1124/vnumap.4452)

(PL) quantum yield (QY), and high photoresistance [2-4]. Recently, many studies have focused on the synthesis of the type-II semiconductor QDs. They were constructed from the two materials for which both the conduction and valence bands of one component lie lower in energy than the corresponding bands of the other component [5, 6]. Type-II QDs have an effective bandgap energy that is smaller than that of either the constituent core or shell. For example, CdTe/CdSe or CdSe/CdTe QDs can emit infrared radiation that is even beyond the bulk band gaps of either CdSe or CdTe, so they can be conveniently used for *in vivo* imaging [7]. Furthermore, the spatial charge separations of electrons/holes between the core/shell and extended absorptions of type-II QDs can be advantageous for photovoltaic applications and lasers [8]. Although there are many potential applications but the optical properties of type-II QDs have not been clearly understood due to the difficulties in making high quality QDs [9].

Since Bawendi's first research in 2003 [10], for the first time, type-II CdTe/CdSe core/shell QDs were successfully prepared by using the colloidal chemical method. Afterwards, a series of type-II core/shell QDs such as CdS/ZnSe [3, 6], CdTe/CdSe [11], CdTe/ZnSe [12], ZnTe/ZnSe [13], and ZnTe/CdSe [14] has been fabricated in recent years. For the above QDs, the type-II CdTe/CdSe core/shell QDs were fabricated more than other QDs, because it can be separated completely electrons and holes between the core and shell layers. The type-II CdTe/CdSe core/shell QDs have emission wavelengths in the visible region and can change in a very wide range when changing core size and shell thickness. The bandgap energy of CdTe/CdSe and CdSe/CdTe QDs are the same, but the physical nature and their applications are different. For the CdTe/CdSe QDs, electrons locate in the shell and holes locate in the core, while the CdSe/CdTe QDs are opposite. Electrons locate in the core of the CdSe/CdTe QDs, which have many potential applications in solar cells and give higher emission efficiency, because electrons are not arrested by traps on the surface of the QDs. Compared with the CdTe/CdSe QDs, the CdSe/CdTe QDs are less studied and fabricated due to the shell containing Te compound. A problem associated with a practical use of CdSe/CdTe QDs is known that the CdTe shell is easily oxidized, which results in reduced chemical stability. Oxidation also reduces quantum yield (QY) and may require incorporation of additional protection layers that isolate the Te-based material from the environment for improved PL QY [7, 11].

In this work, we investigate the crystal structure and optical properties of type-II/type-I CdSe/CdTe/ZnS core/shell/shell QDs and comparison with the traditional type-II CdSe/CdTe core/shell QDs. The type-II characteristic of CdSe/CdTe core/shell QDs were clarified by UV-vis absorption and PL spectra. The formations of the zincblende and core/shell/shell structure were monitored by using Raman scattering (RS) and an X-ray diffractometer. The additional ZnS shell, with large bandgap energy, efficiently confines both electrons and holes in the CdSe/CdTe structure and significantly enhances the indirect radiative recombination at the CdSe core and inner CdTe shell interface. Furthermore, the ZnS shell also helps to enhance PL QY, the optical durability, the chemical stability and separating CdSe/CdTe QDs from the surroundings.

2. Experimental Details

Chemicals

Cadmium oxide (CdO, 99.99%, powder), Zinc oxide (ZnO, 99.99%), 1-octadecene (ODE, 90%), Oleic acid (OA, 90%), Tellurium (Te, 99.99%, powder), Selenium (Se, 99.99%, powder), Toluene (99.8%), Isopropanol (99.7%) and Tri-n-octylphosphine (TOP, 97%) were purchased from Sigma-Aldrich.

Synthesis of CdSe quantum dots

A mixture of CdO (128 mg), OA (3 ml), and ODE (20 ml) in a flask was heated to 260 °C and stirring. A solution of Se (79 mg) and TOP (1ml) in ODE (5ml) was swiftly injected into above hot solution for the growth of CdSe QDs. The fabricated CdSe QDs were purified by centrifuging to remove extra unreacted Cd²⁺ and Se²⁻ ions. The purified CdSe QDs were dissolved in toluene and ODE for using to cover CdTe shell. Note that all of the synthesis processes were performed in nitrogen ambience to avoid oxidation.

Overcoating with CdTe shell

The Te²⁻ precursor was prepared by mixing 128 mg of Te powder, 1mL TOP and 4 ml of ODE in a flask, then heated to 100 °C. The Cd²⁺ (prepared as above) and Te²⁻ precursors solution were swiftly injected into the solution containing CdSe QDs at 250 °C. The growth was carried out for 20 min to grow the CdTe shell. The fabricated CdSe/CdTe QDs were purified and dissolved in toluene and ODE to cover ZnS second shell.

Overcoating with ZnS shell

A mixture of ZnO (81mg), OA (3 ml), and ODE (20 ml) in a flask was heated to 260 °C. S²⁻ precursor was prepared by mixing 32 mg of S powder and 4 ml of ODE in a flask, then heated to 120 °C. Zn²⁺ and S²⁻ precursors solution were swiftly injected into the solution containing CdSe/CdTe QDs at 220 °C and annealing for 20 min to grow the ZnS shell. The fabricated CdSe/CdTe/ZnS QDs were purified and dissolved in toluene for studying the structural and optical properties afterwards.

Characterizations

To study the optical properties, Ultraviolet–visible (UV–vis) absorption spectra were analyzed by using a Jasco V-770 spectrometer (Varian). Raman (RS) and PL spectra were performed on a LABRAM-HR800 spectrometer (Horriba, Jobin Yvon). In our work, excitation power could be changed in the ranges of 0.01–10 mW (using a filter power density). PL decay curves were recorded by a home-built time-resolved PL system with an excitation wavelength of 405 nm. The crystal structure of the fabricated samples was checked using an X-ray diffractometer (Siemens, D5005) equipped with a Cu-K α radiation source. All investigations were carried out at room temperature.

3. Results and Discussion

Firstly, we use an RS spectra to monitor the formation of CdTe and ZnS shells on the CdSe cores. Figure 1 shows the RS spectra of CdSe core, CdSe/CdTe core/shell and CdSe/CdTe/ZnS core/shell/shell QDs were excited by wavelength of 488 nm. For the CdSe core, there are vibration modes peaked at ~ 206 and ~ 412 cm⁻¹, which are associated with the longitudinal optical (1LO_{CdSe} and 2LO_{CdSe}) phonons of CdSe QDs [2, 11]. The 1LO_{CdSe} position of bulk CdSe locates at about 213 cm⁻¹ [11]. The redshift of this mode is ascribed to phonon confinement effects due to the size of CdSe QDs. For CdSe/CdTe core/shell QDs, besides having two phonon modes of CdSe core, we can see third mode at ~ 157 cm⁻¹. It is well known that the phonons vibration at ~ 163 cm⁻¹ is belong to the longitudinal optical phonon of CdTe, which marked as 1LO_{CdTe} [15]. The appearance of the phonon mode at ~ 157 cm⁻¹ evidence that our CdSe/CdTe QDs are well formed in the core/shell structure. The RS spectra of CdSe/CdTe/ZnS QDs shows that, besides 1LO_{CdSe}, 2LO_{CdSe} and 1LO_{CdTe} peaks, there is

an additional mode peaked at $\sim 350\text{ cm}^{-1}$, which is ascribed to the 1LO_{ZnS} phonon mode of the ZnS shell. In particular, with coating ZnS shell layers, the phonon modes 1LO_{CdSe} and 1LO_{CdTe} of CdSe/CdTe/ZnS QDs are shifted about 3 cm^{-1} towards higher wavenumbers, which is ascribed to the lattice strain. The observed results of the phonon modes 1LO_{CdTe} and 1LO_{ZnS} confirm the formation of the core/shell/shell structure in CdSe/CdTe/ZnS QDs.

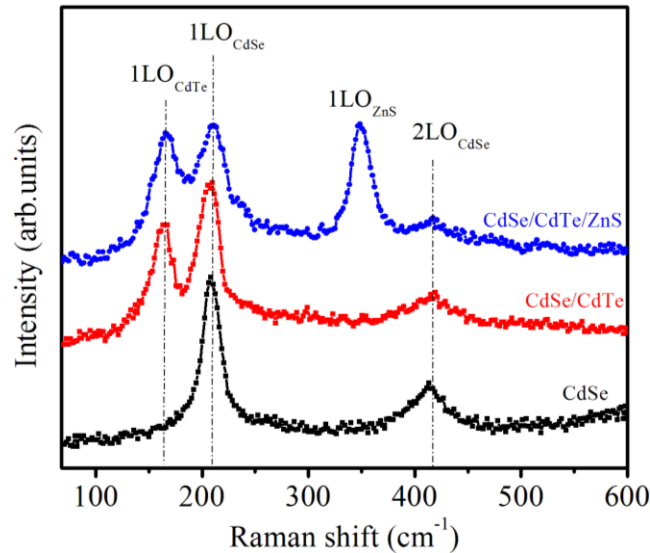


Figure 1. RS spectrum of CdSe, CdSe/CdTe, and CdSe/CdTe/ZnS.

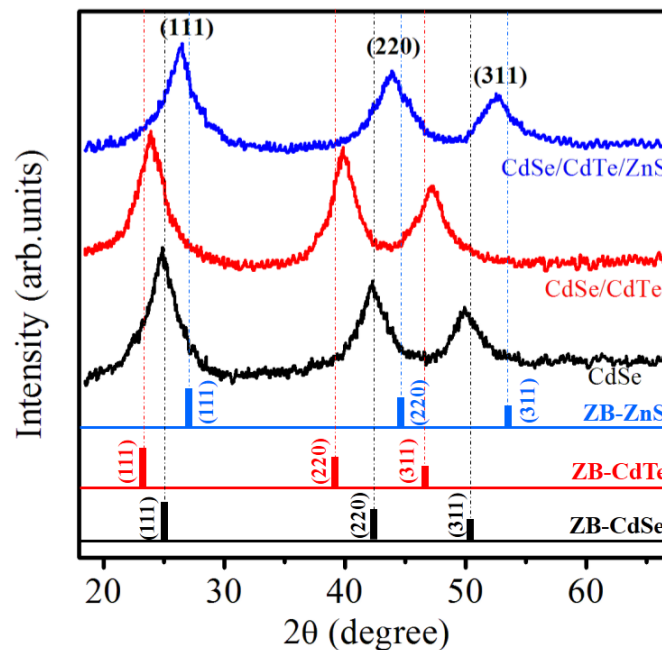


Figure 2. XRD patterns of CdSe, CdSe/CdTe, and CdSe/CdTe/ZnS QDs.

XRD pattern in Figure 2 reveals the crystal structures of CdSe, CdSe/CdTe core/shell, and CdSe/CdTe/ZnS core/shell/shell QDs. The XRD patterns of all samples match with the zinc blende structure and no indication of the hexagonal phase formation, all the peaks match well with the standard Bragg reflections for the cubic structure. The diffraction peaks show broadening phenomena because of the QDs' small sizes. According to Scherrer's formula, crystallite size $D = K\lambda / (B\cos\theta)$ [16], where K is the Scherrer constant, λ is the wavelength (1.5406 Å for Cu-K α radiation), B is the FWHM of the XRD peaks, and θ is the peak position. From the line width analysis of the (111) reflection peak using the Scherrer equation, the average diameter of CdSe QDs is estimated about 5.4 nm, which is in agreement with the result has obtained from the equation of Yu. After the growth of the CdTe shell, the XRD peaks of CdSe/CdTe QDs shift to smaller angles because the CdTe lattice constant (0.648 Å) is bigger than that of cubic CdSe (0.608 Å) [11, 15]. After the further growth of the ZnS shell, the XRD peaks strongly shift to larger angles because the ZnS lattice constant (0.541 Å) is much smaller than that of CdTe. The sustenitive zincblende structure throughout the growth processes of CdTe and ZnS shells are likely due to the surfactant system used. The QDs such as CdTe, CdSe, and CdS synthesized in OA usually have zincblende structure because the ligand OA has a stabilizing effect on this phase [17].

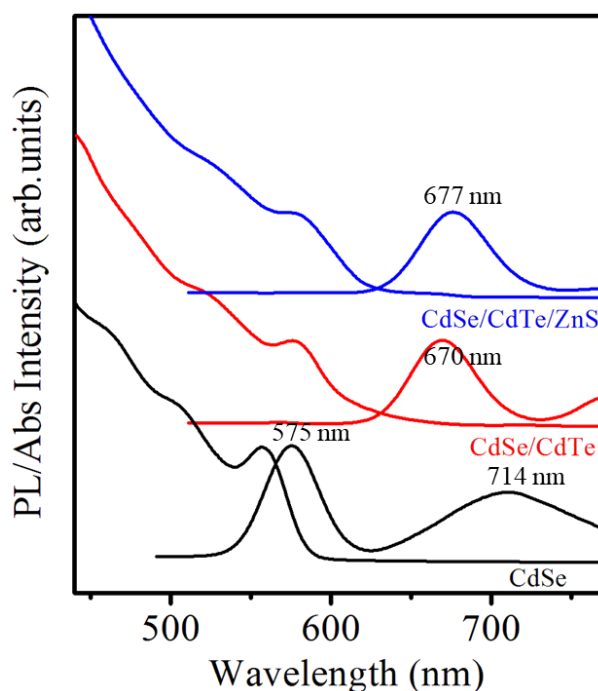


Figure 3. UV-vis absorption and PL spectra of CdSe, CdSe/CdTe, and CdSe/CdTe/ZnS QDs.

Figure 3 displays the absorption (Abs) and PL spectra of CdSe core, CdSe/CdTe core/shell and CdSe/CdTe/ZnS core/shell/shell QDs. For the Abs spectra of CdSe core QDs, one can see clearly the first excitonic absorption peaks at wavelength about 560 nm. The energy of this absorption peak corresponding to the lowest energy transition of $1S_{3/2}(h)$ - $1S(e)$, which can be used to estimate the diameter of the QDs according to Yu's empirical equation [18]. Using the equation of Yu: $D = (1.6122 \times 10^{-9})\lambda^4 - (2.6575 \times 10^{-6})\lambda^3 + (1.6242 \times 10^{-3})\lambda^2 - (0.4277)\lambda + 41.57$, with λ is first excitonic absorption

peak, the size (D) of CdSe core QDs is determined ~ 5 nm. The PL spectra of CdSe QDs shows a peak at ~ 575 nm corresponding to the recombination of the electron in the conduction band and the holes in the valence band, known as excitonic emission. The broadened peak at ~ 714 nm with the lower intensity is assigned to the surface state of QDs [19]. The PL QY of CdSe core QDs is determined of 42.6 %. After the growth of the CdTe shell, Abs spectra of CdSe/CdTe core/shell QDs appears a long absorption tail at long wavelength (from 620 to 700 nm). The long tail and the smeared Abs peaks are considered as a signature of the spatial indirect absorption of the type-II QDs [15, 20]. As the CdTe shell grows on CdSe core, the PL peak red shifts from 575 nm for the CdSe core to 670 nm for type-II CdSe/CdTe core/shell QDs. This redshift is typical characteristics for type-II QDs due to the spatially indirect recombination of the charge carriers at the type-II heterojunction. The similar results were observed previously in studies of the type-I to the type-II transition in CdTe/CdSe [11] or CdS/ZnSe [3, 6] QDs. The PL QY decrease from 42.6 % for CdSe core to 33.4 % for CdSe/CdTe core/shell QDs. The growth of the CdTe shell leads to the decrease of the PL QY due to the significant reduction of the electron-hole function overlap in type-II QDs. Low PL QY has been seen as an intrinsic limitation of type-II QDs, because the slower radiative recombination of indirect excitons should create the favorable conditions for the dominance of nonradiative recombination [21].

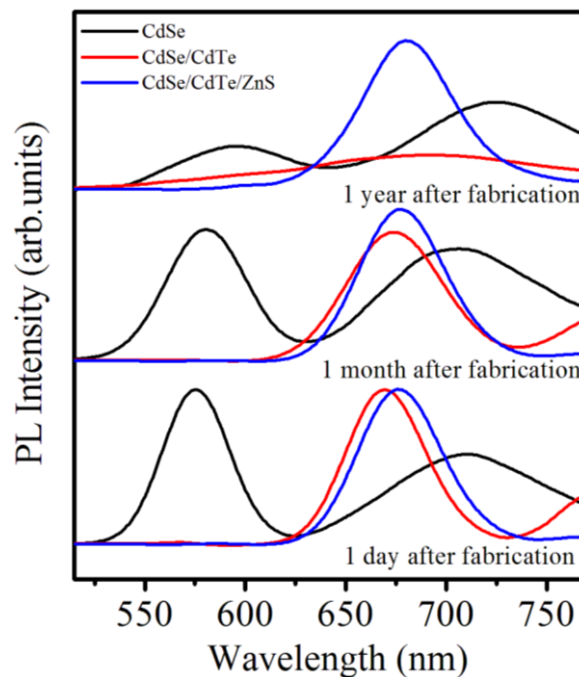


Figure 4. PL spectrum of CdSe, CdSe/CdTe, and CdSe/CdTe/ZnS QDs according to storage time.

When the additional ZnS shell grows on CdSe/CdTe core/shell QDs, the PL peak of CdSe/CdTe/ZnS core/shell/shell slightly redshifts about 7 nm compare to that of CdSe/CdTe core/shell QDs. This was expected because ZnS (3.6 eV) has a very wide bandgap in comparison to CdTe (1.4 eV) that forms the type-I structure with the ZnS shell [2, 7]. As expected, the PL QY of the CdSe/CdTe core/shell QDs was significantly enhanced (up to 48.7 %) upon the growth of the ZnS shell. The research result with CdS/ZnSe QDs also shown that the PL QY of these QDs were improved from about 30% to 60% after the growth of thick ZnS shell [22]. ZnS shell was grown to improve the QY and PL stability of CdSe/CdTe core/shell QDs because the large bandgap semiconductor ZnS

confined the photoexcited excitonics in the CdSe/CdTe core/shell QDs, reduced oxidized, chemical stability, and nonradiative recombinations through the surface defects of CdTe shell was eliminated [7, 22]. It can be seen in Figure 4 that the CdSe/CdTe/ZnS QDs still emitted well after one year of storage under normal conditions, while the CdSe and CdSe/CdTe QDs were almost no longer emitted.

In order to further understand the physical process underlying the spectra feature of the type-I and type-II QDs emission, we measured the decay curves of the excitonic emission of three samples, which

are shown in Figure 5. The PL decay can be fitted to a triexponential function: $I(t) = \sum_{i=1}^3 A_i e^{-\frac{t}{\tau_i}}$ [6,

15], where A_i and τ_i are the magnitude and lifetime of the i_{th} component, respectively. The τ_i values are strongly dependent on various crystal sizes and morphologies. Average lifetime $\langle \tau \rangle$ can be determined

from the A_i and τ_i values as: $\langle \tau \rangle = \frac{\sum_{i=1}^3 A_i \tau_i^2}{\sum_{i=1}^3 A_i \tau_i}$ [6, 15]. The measured $\langle \tau \rangle$ are 12.7 ns for the CdSe

core, 56.2 ns for the CdSe/CdTe core/shell, and 47.4 ns for the CdSe/CdTe/ZnS core/shell/shell. The appreciable increase in the excitonic lifetime observed for type-II CdSe/CdTe QDs compare to the CdSe cores is primarily due to the spatial separation of the electron and hole, and the increase of the nonradiative decay rates, since it is accompanied by a significant decrease of the PL QY (from 42.6 % down 33.4 %). A further growth of the ZnS shell leads to decreasing the exciton lifetime suitable for increasing the PL QY of CdSe/CdTe/ZnS QDs (from 33.4 % to 48.7 %).

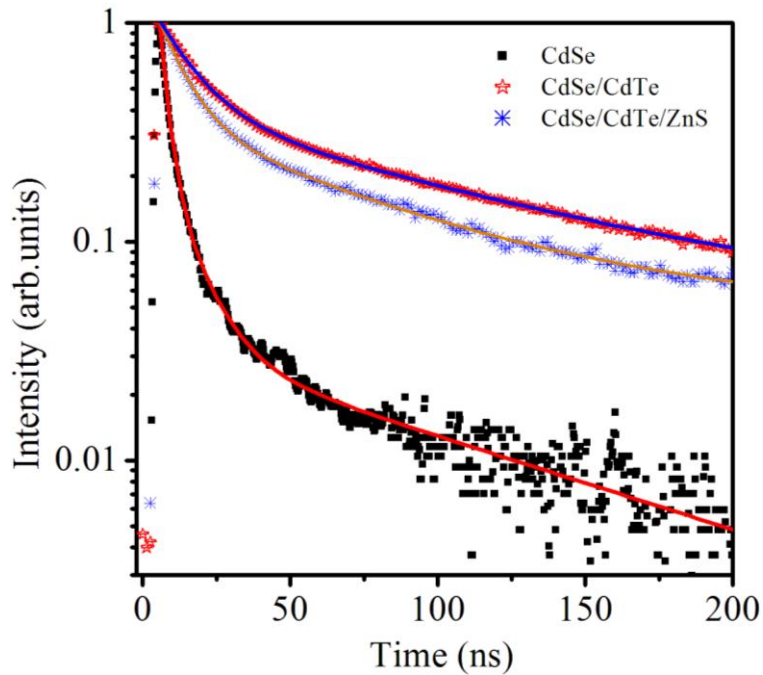


Figure 5. Time-resolved PL decays of CdSe, CdSe/CdTe, and CdSe/CdTe/ZnS QDs.

In an attempt to investigate the emission dynamics, we changed excitation power from 0.01 to 10 mW, and studied their influences on the PL properties of CdSe, CdSe/CdTe and CdSe/CdTe/ZnS QDs. The PL spectrum shown in Figure 6(a–c) show that though the spectral shape remains unchanged but the spectral parameters vary remarkably. The dependence of integrated emission intensity on the

excitation power of samples is observed in the Figure 7a. The integrated emission intensity versus the excitation power obeys a law of $I \propto P^k$, where k is a power factor reflecting different natures of the emissions. For CdSe QDs, $k=0.97$ (~ 1), which is expected for the transitions associated with free excitonics [23]. This transition processes are related to the direct recombination of electrons and holes confined in CdSe core. For CdSe/CdTe and CdSe/CdTe/ZnS QDs, k takes the values of 1.36 and 1.42, respectively. The values of $k > 1$ is due to different natures of the emissions, they could be for bound excitonics, donor-acceptor pairs [24], and the bounding of excitonics to isoelectronic defects [25]. These k values associated to the emission of the type-II QDs, which related to the indirect recombination of the spatially separate electrons and holes between the core and the shell.

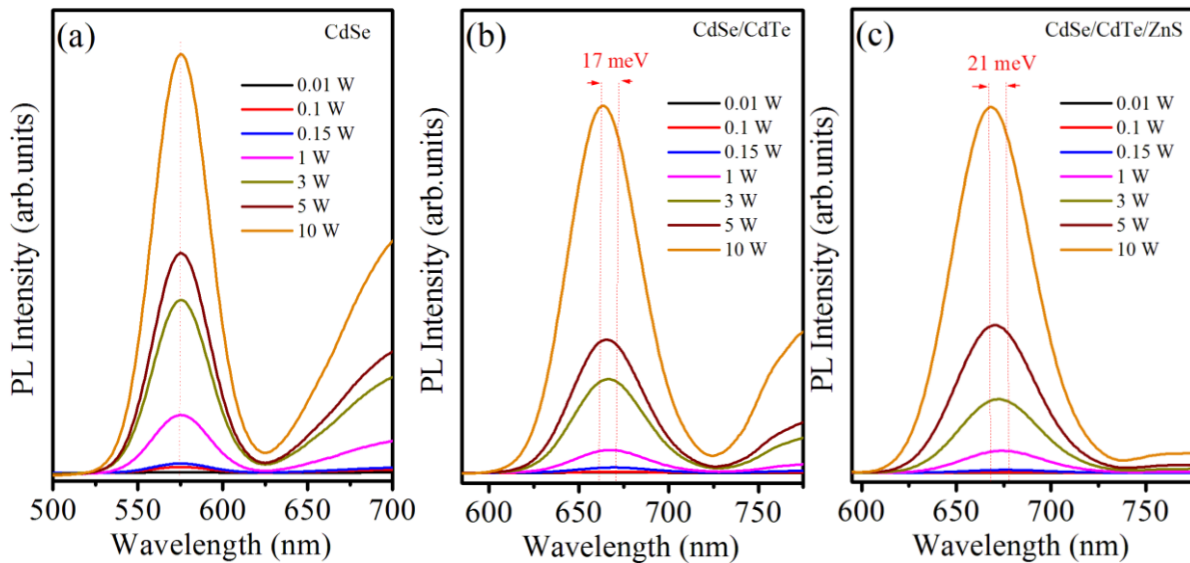


Figure 6. PL spectrum of CdSe, CdSe/CdTe, and CdSe/CdTe/ZnS QDs when excitation power increases from 0.01 - 10 mW.

The results in Figure 6 show the emission peaks of CdSe QDs were unchanged, while that of CdSe/CdTe and CdSe/CdTe/ZnS QDs were shifted towards high energies as increasing the excitation power. It is well known that the type-II QDs show a characteristic of the blueshift of PL spectra with increasing excitation power, while the blueshift is not observed in type-I QDs [6, 15]. The blueshift phenomena of PL in type-II QDs has been explained by several mechanisms, such as the capacitive charging (CC) [26], state filling (SF) [27], and band bending (BB) [15, 28]. The CC effect is caused by the repulsion interaction force between the same electric charge (electron-electron or hole - hole), which is much larger than the attraction interaction force between electrons and holes. The result of this effect is that the emission energy is proportional to the square root of the excitation power ($E \sim P^{1/2}$). The BB effect is a consequence of the bending of the energy region of type-II QDs. The separation of carriers are generated by optical excitation into different spatial regions of type-II core/shell QDs. When the excitation power is high, the carriers will intensively concentrate at the interface to produce the internal electric field, and cause the bending of conduction and valence bands of the semiconductor components. For BB effect, the emission energy is linearly proportional to the cube root of the excitation power ($E \sim P^{1/3}$). Analyzed PL data are shown Figure 7b. For CdSe cores, the dependence of the emission energy and the excitation power is constant. However, the situation became different for the CdSe/CdTe core/shell and CdSe/CdTe/ZnS core/shell/shell samples. The PL

spectrum of CdSe/CdTe and CdSe/CdTe/ZnS show a clear blueshift about 17 and 21 meV, respectively, and its PL peak has is the linear relationship with the third root of excitation power. This result proves that the BB effect is the cause for the blueshift of PL peaks as increasing excitation power. The BB effect has also been observed with the CdTe/CdSe [15] and CdS/ZnSe [6], however the blueshift energy is different depending on the sample nature. The BB effect of CdSe/CdTe/ZnS QDs is more strongly than that of CdSe/CdTe QDs because the ZnS shell has good passivation of the defects on surface of CdSe/CdTe QDs, which is suitable for the QY enhancement of CdSe/CdTe/ZnS QDs.

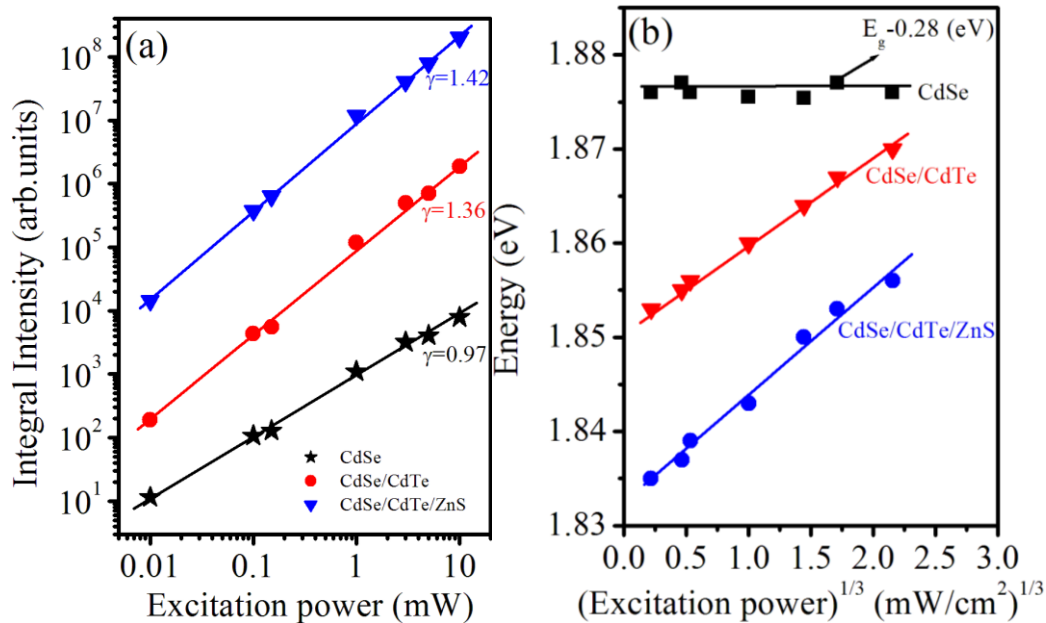


Figure 7. (a) Dependence of integrated PL intensity on the excitation power.
(b) Dependence of PL peak energy on the cube root of excitation power.

4. Conclusion

The CdSe, type-II CdSe/CdTe core/shell and type-II/type-I CdSe/CdTe/ZnS core/shell/shell QDs were synthesized in ODE solvent. The formation of the core/shell and core/shell/shell structures was proved by using RS. XRD reveal that all samples crystallize in the cubic phase with zinc-blende structure. The typical characteristics of spatially indirect recombination for type-II QDs were observed through Abs and PL spectroscopy. The ZnS shell significantly enhanced the PL QY, the optical durability, the chemical stability and separating CdSe/CdTe QDs from the surroundings. The effect of excitation power on the PL properties of the CdSe core, CdSe/CdTe and CdSe/CdTe/ZnS QDs has been investigated.

Acknowledgments

This research is funded by Vietnam National Foundation for Science and Technology Development (NAFOSTED) under grant number 103.02-2017.350.

References

- [1] A. Nemchinov, M. Kirsanova, N.H. Kasakarage, M. Zamkov, Synthesis and Characterization of Type II ZnSe/CdS Core/Shell Nanocrystals, *J. Phys. Chem. C*. 112 (2008) 9301–9307. <https://doi.org/10.1021/jp801523m>.
- [2] W. Zhang, G. Chen, J. Wang, B.C. Ye, X. Zhong, Design and Synthesis of Highly Luminescent Near-Infrared-Emitting Water-Soluble CdTe/CdSe/ZnS Core/Shell/Shell Quantum Dots, *Inorg. Chem.* 48 (2009) 9723–9731. <https://doi.org/10.1021/ic9010949>.
- [3] H.T. Van, N.X. Ca, N.T. Hien, P.M. Tan, T.L. Phan, L.D. Thanh, P.V. Do, N.Q. Bau, V.T.K. Lien, Tunable dual emission in type-I/type-II CdSe/CdS/ZnSe nanocrystals, *J. Alloy. Compd.* 791 (2019) 144–151. <https://doi.org/10.1016/j.jallcom.2019.03.333>.
- [4] C. Zhang, S. Liu, X. Liu, F. Deng, Y. Xiong, F.C. Tsai, Incorporation of Mn²⁺ into CdSe quantum dots by chemical bath co-deposition method for photovoltaic enhancement of quantum dot-sensitized solar cells, *R. Soc. Open. Sci.* 5 (2018) 171712. <https://doi.org/10.1098/rsos.171712>.
- [5] N.H. Kasakarage, P.Z. Khoury, A.N. Tarnovsky, M. Kirsanova, I. Nemitz, A. Nemchinov, M. Zamkov, Ultrafast Carrier Dynamics in Type II ZnSe/CdS/ZnSe Nanobarels, *ACS Nano*. 4 (2010) 1837–1844. <https://doi.org/10.1021/nn100229x>.
- [6] N.X. Ca, V.T.K. Lien, P.M. Tan, N.T. Hien, V.X. Hoa, T.T.K. Chi, N.X. Truong, V.T.K. Oanh, N.T.M. Thuy, Tunable photoluminescent Cu-doped CdS/ZnSe type-II core/shell quantum dots, *J. Lumin.* 215 (2019) 116627. <https://doi.org/10.1016/j.jlumin.2019.116627>.
- [7] H.Q. Huang, J.L. Liu, B.F. Han, C.C. Mi, S.K. Xu, Cell labeling and cytotoxicity of aqueously synthesized CdTe/CdS/ZnS core-shell-shell quantum dots by a water bath-hydrothermal method, *J. Lumin.* 132 (2012) 1003. <https://doi.org/10.1016/j.jlumin.2011.11.010>.
- [8] J. Bang, J. Park, J.H. Lee, N. Won, J. Nam, J. Lim, B.Y. Chang, H.J. Lee, B. Chon, J. Shin, J.B. Park, J.H. Choi, K. Cho, S.M. Park, T. Joo, S. Kim, ZnTe/ZnSe (Core/Shell) Type-II Quantum Dots: Their Optical and Photovoltaic Properties, *Chem. Mater.* 22 (2010) 233–240. <https://doi.org/10.1021/cm9027995>.
- [9] C.H. Wang, T.T. Chen, K.W. Tan, Y.F. Chen, Photoluminescence properties of CdTe/CdSe core-shell type-II quantum dots, *J. Appl. Phys.* 99 (2006) 123521. <https://doi.org/10.1063/1.2207721>.
- [10] S. Kim, B. Fisher, H.J. Eisler, M.G. Bawendi, Type-II Quantum Dots: CdTe/CdSe(Core/Shell) and CdSe/ZnTe(Core/Shell) Heterostructures, *J. Am. Chem. Soc.* 125 (2003) 11466. <https://doi.org/10.1021/ja0361749>.
- [11] G.R. Bhand, N.B. Chaurse, Synthesis of CdTe, CdSe and CdTe/CdSe core/shell QDs from wet chemical colloidal method, *Mater. Sci. Semicond. Process.* 68 (2017) 279–287. <https://doi.org/10.1016/j.mssp.2017.06.033>.
- [12] N.H. Kasakarage, N.P. Gurusinghe, M. Zamkov, Blue-Shifted Emission in CdTe/ZnSe Heterostructured Nanocrystals, *J. Phys. Chem. C*. 113 (2009) 4362–4368. <https://doi.org/10.1021/jp8106843>.
- [13] S.M. Fairclough, E.J. Tyrrell, D.M. Graham, P.J.B. Lunt, S.J.O. Hardman, A. Pietzsch, F. Hennies, J. Moghal, W. R. Flavell, A.A.R. Watt, J.M. Smith, Growth and Characterization of Strained and Alloyed Type-II ZnTe/ZnSe Core-Shell Nanocrystals, *J. Phys. Chem. C*. 116 (2012) 26898–26907. <https://doi.org/10.1021/jp3087804>.
- [14] Z. Jiang, D.F. Kelley, S. Krastanov, Stranski–Krastanov Shell Growth in ZnTe/CdSe Core/Shell Nanocrystals, *J. Phys. Chem. C*. 117 (2013) 6826–6834. <https://doi.org/10.1021/jp4002753>.
- [15] N.X. Ca, N.T. Hien, N.T. Luyen, V.T.K. Lien, L.D. Thanh, P.V. Do, N.Q. Bau, T.T. Pham, Photoluminescence properties of CdTe/CdTeSe/CdSe core/alloyed/shell type-II quantum dots, *J. Alloy. Compd.* 787 (2019) 823–830. <https://doi.org/10.1016/j.jallcom.2019.02.139>.
- [16] N.X. Ca, H.T. Van, P.V. Do, L.D. Thanh, P.M. Tan, N.X. Truong, V.T.K. Oanh, N.T. Binh, N.T. Hien, Influence of precursor ratio and dopant concentration on the structure and optical properties of Cu-doped ZnCdSe-alloyed quantum dots, *RSC Adv.* 10 (2020) 25618. <https://doi.org/10.1039/D0RA04257A>.
- [17] P.T. Tho, N.D. Vinh, H.T. Van, P.M. Tan, V.X. Hoa, N.T. Kien, N.T. Hien, N.T.K. Van, N.X. Ca, Effects of chemical affinity and injection speed of Se and Te precursors on the development kinetic and optical properties of ternary alloyed CdTe_{1-x}Se_x nanocrystals, *J. Phys. Chem. Solid.* 139 (2020) 109332. <https://doi.org/10.1016/j.jpcs.2020.109332>.

- [18] W.W. Yu, L. Qu, W. Guo, X. Peng, Experimental determination of the extinction coefficient of CdTe, CdSe, and CdS nanocrystals, *Chem. Mater.* 15 (2003) 2854-2860. <https://doi.org/10.1021/cm034081k>.
- [19] H.T. Van, N.D. Vinh, P.M. Tan, U.T.D. Thuy, N.X. Ca, N.T. Hien, Synthesis and optical properties of tunable dual emission copper doped CdTe_{1-x}Se_x alloy nanocrystals, *Optic. Mater.* 97 (2019) 109392. <https://doi.org/10.1016/j.optmat.2019.109392>.
- [20] B. Blackman, D.M. Battaglia, T.D. Mishima, M.B. Johnson, X. Peng, Control of the Morphology of Complex Semiconductor Nanocrystals with a Type II Heterojunction, Dots vs Peanuts, by Thermal Cycling, *Chem. Mater.* 19 (2007) 3815–3821. <https://doi.org/10.1021/cm0704682>.
- [21] P.T.K. Chin, C.M. Donega, S.S.V. Bavel, S.C.J. Meskers, N.A.J.M. Sommerdijk, R.A.J. Janssen, Highly Luminescent CdTe/CdSe Colloidal Heteronanocrystals with Temperature-Dependent Emission Color, *J. Am. Chem. Soc.* 129 (2007) 14880-14886. <https://doi.org/10.1021/ja0738071>.
- [22] J.Z. Niu, H. Shen, C. Zhou, W. Xu, X. Li, H. Wang, S. Lou, Z. Du, L.S. Li, Controlled synthesis of high quality type-II/type-I CdS/ZnSe/ZnS core/shell1/shell2 nanocrystals, *Dalton Trans.* 39 (2010) 3308–3314. <https://doi.org/10.1039/B922130A>.
- [23] V.I. Klimov, S.A. Ivanov, J. Nanda, M. Achermann, I. Bezel, J.A. McGuire, A. Piryatinski, Single-exciton optical gain in semiconductor nanocrystals, *Nat. Commun.* 24 (2007) 441-447. <https://doi.org/10.1038/nature05839>
- [24] F. Luckert, M.V. Yakushev, C. Faugeras, A.V. Karotki, A.V. Mudryi, R.W. Martin, Excitation power and temperature dependence of excitons in CuInSe₂, *J. Appl. Phys.* 111 (2012) 093507. <https://doi.org/10.1063/1.4709448>.
- [25] J. Weber, W. Schmid, R. Sauer, Localized exciton bound to an isoelectronic trap in silicon, *Phys. Rev. B.* 2 (1980) 2401. <https://doi.org/10.1103/PhysRevB.21.2401>.
- [26] P.D. Hodgson, R.J. Young, M.A. Kamarudin, P.J. Carrington, A. Krier, Q.D. Zhuang, E.P. Smakman, P.M. Koenraad, M. Hayne, Blueshifts of the emission energy in type-II quantum dot and quantum ring nanostructures, *J. Appl. Phys.* 114 (2013) 073519. <https://doi.org/10.1063/1.4818834>.
- [27] K. Suzuki, R.A. Hogg, Y. Arakawa, Structural and optical properties of type II GaSb/GaAs self-assembled quantum dots grown by molecular beam epitaxy, *J. Appl. Phys.* 85 (1999) 8349. <https://doi.org/10.1063/1.370622>.
- [28] H.T. Van, N.D. Vinh, N.X. Ca, N.T. Hien, N.T. Luyen, P.V. Do, N.V. Khiem, Effects of ligand and chemical affinity of S and Se precursors on the shape, structure and optical properties of ternary CdS_{1-x}Se_x alloy nanocrystals, *Mater. Lett.* 264 (2020) 127387. <https://doi.org/10.1016/j.matlet.2020.127387>.